Gallery of Fluid Motion

Visualizations of a methane/diesel RCCI engine using PeleC and PeleLMeX

Nicholas T. Wimer,* Lucas Esclapez, Nicholas Brunhart-Lupo, Marc Henry de Frahan, Mohammad Rahimi, Malik Hassanaly, Jon Rood, Shashank Yellapantula, Hariswaran Sitaraman, Bruce Perry, Michael Martin, Olga Doronina, Sreejith N. Appukuttan, Martin Rieth,† and Marc Day

National Renewable Energy Laboratory, 15013 Denver West Pkwy, Golden, Colorado, USA

(Received 3 June 2023; published 17 November 2023)

This paper is associated with a video winner of a 2022 American Physical Societys Division of Fluid Dynamics (DFD) Milton van Dyke Award for work presented at the DFD Gallery of Fluid Motion. The original video is available online at the Gallery of Fluid Motion, https://doi.org/10.1103/APS.DFD.2022.GFM.V0076

DOI: 10.1103/PhysRevFluids.8.110511

New fuel injection strategies have emerged for compression-ignition (CI) engines in an effort to reduce the NO_x and soot emissions that are traditionally associated with CI engines. These so-called advance compression ignition (ACI) strategies take many forms, with one of the more prominent involving a dual-fuel approach that carefully balances a mixture of low-reactivity fuel (LRF) and high-reactivity fuel (HRF). Reactivity-controlled compression ignition (RCCI) [1] operates by directly injecting a HRF (e.g., diesel) though one or more pulses into a homogeneous mixture of an oxidizer and a LRF (e.g., methane). The LRF autoignites at a higher temperature and pressure than the HRF, such that the premixed LRF-air combination will not autoignite without the assistance of either a spark or a separate ignition process. Once the HRF is injected into the combustion chamber, the ambient conditions are amenable to autoignition of the HRF. The HRF autoignites and the expanding ignition kernels subsequently ignite the surrounding LRF. Through careful control of the injection timing and dual-fuel properties, RCCI enables the burning of the fuel mixture in a combustion regime that does not readily produce NO_x or soot emissions, called the low-temperature combustion (LTC) regime [2]. This strategy requires a comprehensive understanding of the combustion dynamics of turbulent flows coupled with the detailed chemical kinetics of dual-fuel reactions. Due to this complexity, high-resolution numerical simulations are vital in providing physical insight, either by allowing for testing and screening of coupled injection strategies with novel fuel blends and engine geometries or through the development of reduced order models for the approximation of engine dynamics in the design process.

In this work, we develop and employ two exascale-ready computational fluid dynamics (CFD) packages [3], PeleC [4] and PeleLMeX [5], on an RCCI engine setup and create cutting-edge visualizations to provide insight into the onset of the turbulent combustion process. Both codes use adaptive mesh refinement (AMR) on a Cartesian grid with embedded boundaries (EBs) to model complex geometries. In PeleC we solve the fully compressible Navier-Stokes equations,

*nwimer@nrel.gov

†Present address: Sandia National Laboratory.

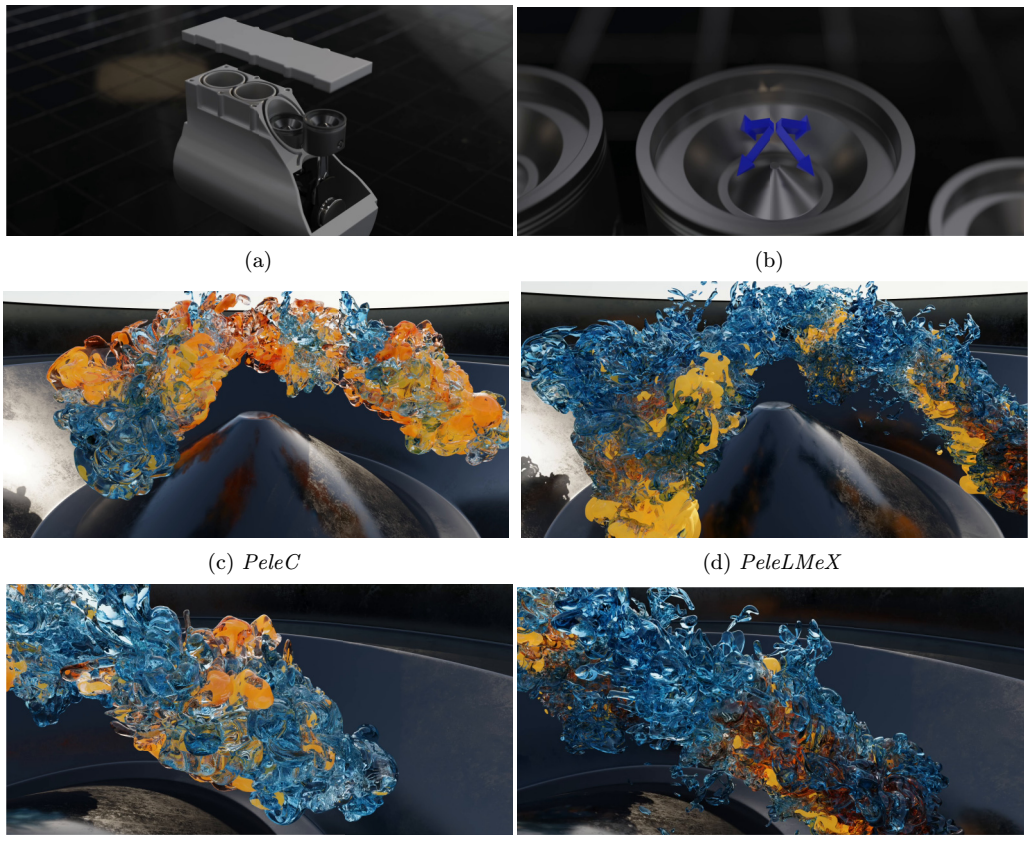

(a) (b)

(c) *PeleC* (d) *PeleLMeX*

(e) *PeleC* (f) *PeleLMeX*

FIG. 1. (a) 3D representation of a four-cylinder CI engine; (b) the piston-bowl geometry showing the four discrete diesel injections into the methane filled piston bowl; (c), (d) yellow/red isosurfaces show temperature hot spots indicating the start of combustion in PeleC and PeleLMeX; (e), (f) close up of a single jet showing the first ignition kernels which form along the shear interface between the diesel jet and methane fuel background in PeleC and PeleLMeX. Please refer to the full video at https://doi.org/10.1103/APS.DFD.2022.GFM.V0076

while in PeleLMeX we solve the low-Mach version of the Navier-Stokes equations. In both codes we use a detailed chemical reaction mechanism to model the combustion process of the two fuels. For visualization, we use the open-source cinematic package Blender to visualize iso-surfaces of fuel mass fraction and temperature, highlighting regions of initial combustion. While we examine an RCCI engine setup here, these codes are equally applicable for a wide range of reacting flow problems and other engine geometries.

The geometry simulated here is a representative piston-bowl/cylinder geometry as shown in Fig. 1(a). The computational domain represents the cylinder volume as the piston reaches the top of its stroke. The cylinder is initially filled with a homogeneous methane/air mixture at an equivalence ratio of $\phi = 0.5$, temperature 900 K, and 60 atm pressure. The velocity field is initialized at a low-level turbulent intensity to approximate swirl from the piston-bowl geometry. Diesel fuel is direct injected into the cylinder from the top of the domain via four discrete jets as shown in Fig. 1(b). Each of the simulations resolves the jet structure through AMR, selectively refined based on temperature gradient and vorticity magnitude. The simulations use up to four grid levels to resolve the physical scale down to approximately 6.8 μm using in excess of two billion computational cells. The use of AMR allows for the extremely fine resolution of the computational

domain in the regions of turbulent mixing and the onset of combustion reaching a fidelity that would otherwise be computationally intractable with uniform grid spacing. Since the simulation is highly resolved, we do not include an explicit subgrid scale turbulence model in these simulations.

Figures 1(c)–1(d) and 1(e)–1(f) show the fuel streams after they have developed and partially mixed with the surrounding hot methane-air mixture. These images are visualizing isosurfaces of diesel mass fraction in blue and temperature hotspots in yellow/red. Figures 1(c) and 1(d) show the development of the fuel jets in both PeleC and PeleLMeX, respectively, at the initial onset of ignition. From the visualizations, we are able to see that the structures in the four jets are different due to the nonhomogenous turbulent mixing. Additionally, we see that the ignition timing is different between the two codes which highlights the impact of compressible effects on the early onset of autoignition. Figures 1(e) and 1(f) show a close up of a single fuel jet for both PeleC and PeleLMeX, respectively. Here the yellow/red isosurfaces highlight the very first ignition kernels that form at the start of the combustion process. From these visualizations we see that the start of ignition occurs along the shear interface between the diesel and methane fuels and is scattered along the interface for both simulations. These results highlight the importance of the numerical scheme in the turbulent mixing processes when performing simulations of autoignition dependent systems such as in CI engines.

Both versions of the Pele codes show similar development of the fuel jets and locations of the onset of autoignition. Nevertheless, there are distinct visual differences between the two results which are the result of differences in the onset of autoignition. RCCI is highly sensitive to turbulent mixing processes and the subsequent onset of the first ignition kernel. The smallest differences due to numerical scheme can influence the onset of ignition and cascade into differences in results, which can be seen here. These simulations represent a benchmark for high-resolution numerical simulations of a real-world RCCI engine setup, resolving down to scales previously not seen in a full three dimensional RCCI simulation. In this work we have shown that it is now possible to perform near-direct numerical simulation (DNS) levels of CFD of a real-world three-dimensional, complex chemistry, RCCI engines using the Pele suite of codes. By incorporating this level of high-resolution numerical simulations into the design process, engine manufacturers will save valuable time and resources during the co-optimization process of engine geometry and fuels. Future work empowered by these computational tools can explore the complex interaction of novel fuel blends and also be used to develop subgrid scale models to improve lower fidelity simulations.

This research was supported by the Exascale Computing Project (17-SC-20-SC), a collaborative effort of the U.S. Department of Energy Office of Science and the National Nuclear Security Administration. This research used resources of the Oak Ridge Leadership Computing Facility, which is a DOE Office of Science User Facility supported under Contract No. DE-AC05-00OR22725 and computing resources sponsored by the Department of Energy's Office of Energy Efficiency and Renewable Energy and located at the National Renewable Energy Laboratory. This work was authored in part by employees of the National Renewable Energy Laboratory, operated by Alliance for Sustainable Energy, LLC, for the U.S. Department of Energy (DOE) under Contract No. DE-AC36-08GO28308. The views expressed in the article do not necessarily represent the views of the DOE or the U.S. Government.

[1] D. Splitter, R. D. Reitz, and R. Hanson, High efficiency, low emissions RCCI combustion by use of a fuel additive, SAE Int. J. Fuels Lubr. **3**, 742 (2010).

[2] R. D. Reitz and G. Duraisamy, Review of high efficiency and clean reactivity controlled compression ignition (RCCI) combustion in internal combustion engines, Prog. Energy Combust. Sci. **46**, 12 (2015).

[3] M. Day, L. Esclapez, M. Henry de Frahan, J. Rood, H. Sitaraman, N. Wimer, R. Grout, and J. Chen, Pele: An exascale-ready suite of combustion codes, Tech. Rep. PR-2C00-82880, National Renewable Energy Lab. (NREL) (2022).

[4] M. T. Henry de Frahan, J. S. Rood, M. S. Day, H. Sitaraman, S. Yellapantula, B. A. Perry, R. W. Grout, A. Almgren, W. Zhang, J. B. Bell, and J. H. Chen, PeleC: An adaptive mesh refinement solver for compressible reacting flows, Int. J. High Perform. Comput. Appl. **37**, 115 (2023).

[5] L. Esclapez, M. Day, B. John, A. Felden, C. Gilet, R. Grout, M. Henry de Frahan, E. Motheau, A. Nonaka, L. Owen, B. Perry, J. Rood, N. Wimer, W. Zhang, PeleLMeX: An AMR low Mach number reactive flow simulation code without level sub-cycling, J. Open Source Softw. **8**, 5450 (2023).